Available online at www.sciencedirect.com
SCIENCE DIRECT
Polymer 47 (2006) 2434–2441
polymer
www.elsevier.com/locate/polymer

High flux ultrafiltration membranes based on electrospun nanofibrous PAN scaffolds and chitosan coating

Kyunghwan Yoon, Kwangsok Kim, Xuefen Wang, Dufei Fang, Benjamin S. Hsiao *, Benjamin Chu *

Department of Chemistry, Stony Brook University, Stony Brook, NY 11794-3400, USA

Received 29 November 2005; received in revised form 5 January 2006; accepted 13 January 2006
Available online 23 February 2006

Abstract

Conventional ultrafiltration (UF) or nanofiltration (NF) filters for water treatments are based on porous membranes, typically manufactured by the phase immersion method. The torturous porosity in these membranes usually results in a relatively low flux rate. In this study, we demonstrated a new type of high flux UF/NF medium based on an electrospun nanofibrous scaffold (e.g. polyacrylonitrile, PAN) coupled with a thin top layer of hydrophilic, water-resistant, but water-permeable coating (e.g. chitosan). Such nanofibrous composite membranes can replace the conventional porous membranes and exhibit a much higher flux rate for water filtration. The interconnected porosity of the non-woven nanofibrous scaffold can be controlled partially by varying the fiber diameter (from about 100 nm to a few micrometers) through the electrospinning processing. The example membrane, containing an electrospun PAN scaffold with an average diameter from 124 to 720 nm and a porosity of about 70%, together with a chitosan top layer having a thickness of about 1 μm, although not yet fully optimized, exhibited a flux rate that is an order magnitude higher than commercial NF membranes in 24 h of operation, while maintaining the same rejection efficiency (>99.9%) for oily waste-water filtration.

Keywords: Ultrafiltration; Nanofiltration; High flux

1. Introduction

In the non-woven fiber industry, one of the fastest growing segments is in filtration applications. Traditionally, wet-laid, melt-blown and spun-bonded non-woven articles, containing micron-size fibers, are most popular for these applications because of the low cost, easy processibility and good filtration efficiency [1,2]. Their applications in filtration can be divided into two major areas: air filtration and liquid filtration. In air filtration, non-woven articles have been used as coalescing filter media [3], dust collector [4], and protective clothing with coatings of selective agents [5]. In liquid filtration, non-woven articles have been used mostly as substrates to support porous membranes for ultrafiltration (UF, that can exclude particle size larger than 100 nm) or nanofiltration (NF, that can exclude particle size larger than a few nanometers) [6].

Recently, electrospun fibers, with diameters 10–100 times smaller than those of non-woven articles (melt-blown and spun-bond filaments), have shown significantly improved efficiency in air filtration [7,8] because of their higher effective porosity and larger surface area to volume ratio. In addition to air filtration, electrospun articles have been demonstrated in many other applications, such as biological substrates (scaffolds for tissue regeneration, immobilized enzymes and catalyst systems, wound dressing articles, artificial blood vessels and materials for prevention of post-operative induced adhesions) [9–11], optical [12] and chemical sensors [13] as well as electrical conductors [14], just to name a few.

One unique feature in electrospinning is its capability to control the fiber diameter (from tens of nanometers to a few micrometers) by varying processing variable(s), such as solution concentration, applied voltage, fluid flow rate, surface tension, etc. [15,16]. The change in fiber diameter provides an opportunity to fine-tune the membrane porosity that also depends on the membrane thickness. The pores in a non-woven

* Corresponding authors. Tel.: +1 631 632 7793 (B.S. Hsiao), Tel. +1 631 632 7928 (B. Chu); fax: +1 631 632 6518.
E-mail addresses: bhsiao@notes.cc.sunysb.edu (B.S. Hsiao), bchu@notes.cc.sunysb.edu (B. Chu).

0032-3861/$ - see front matter © 2006 Elsevier Ltd. All rights reserved.
doi:10.1016/j.polymer.2006.01.042

structure (i.e. the empty space) are highly interconnected and should be particularly suitable for fluid filtration under hydraulic pressures, as the pores cannot be entirely blocked by particles that have penetrated into the membrane. For liquid filtration, porous polymeric membranes manufactured by conventional methods have their intrinsic limitations, e.g. low-flux and high-fouling performance, due to the geometrical structure of pores and the corresponding pore size distribution, for example, produced by the phase immersion method [17] and undesirable macro-void formation across the whole membrane thickness [18]. It appears that the nanofibrous membranes produced by electrospinning can overcome some of these limitations.

Conventional UF or NF media are all based on multi-layer composite structures [19], containing an asymmetric porous membrane to provide filtration functions and a non-woven fibrous support with large fiber diameters of the order of several microns to provide mechanical strength or structure integrity. Now, we have demonstrated a new concept to fabricate high flux UF media (which is also an effective NF media as it can exclude particles with sizes of a few nanometers) [20,21], involving the use of porous electrospun nanofibrous scaffolds to replace the flux-limiting asymmetric porous membrane. The demonstrated systems consisted of a three-tier composite structure: (1) a 'non-porous' hydrophilic top-layer coating (it is non-porous to particles but porous to water) based on crosslinked poly(vinyl alcohol) (PVA), polyether-*b*-polyamide copolymer (Pebax) or their nanocomposites with surface-oxidized multi-walled carbon nanotube (MWNT), (2) an electrospun nanofibrous substrate mid-layer (crosslinked PVA), and (3) a conventional non-woven microfibrous support (melt blown polyethylene terephthalate (PET) mat). These systems, even without being optimized, exhibited an increase in the flux rate by a substantial factor (from a few to greater than ten times per effective macroscopic surface area) over the best-known existing filters to our knowledge, while keeping the same filtration efficiency. However, it is also apparent that the relatively weak mechanical stability of crosslinked-PVA (in the electrospun nanofibrous scaffold support or/and the top coating) in aqueous conditions could limit the long-term operation. To overcome this problem, we have examined the use of a more hydrophobic and mechanical stable polymer, polyacrylonitrile (PAN), as a nanofibrous support and chitosan as a top hydrophilic coating layer.

PAN has been selected as the material for electrospun membranes for two reasons. (1) PAN has been widely used for ultrafiltration [22], nanofiltration [23], and reverse osmosis [24] due to its good solvent resistance. (2) PAN has also been electrospun into precursor form to fabricate carbon nanofibers [25], where the electrospun fiber diameter has been shown to vary from hundreds of nanometers to several micrometers [26]. In this study, the PAN nanofibrous scaffold was used to support a top coating layer based on chitosan. Chitosan is a hydrophilic biopolymer. It is insoluble in neutral pH conditions [27] and thus is water-resistant but water-permeable. It has been used for anti-fouling enhancement of filtration membranes

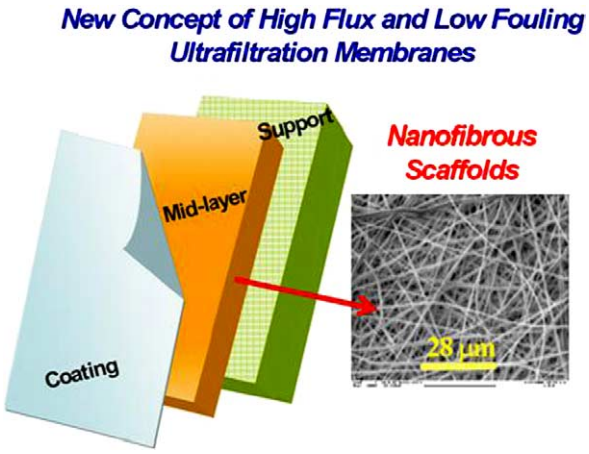

Fig. 1. Three-tier approach to fabricate high flux and low-fouling ultrafiltration membranes.

[22,28,29]. The schematic diagram of the three-tier composite membranes is illustrated in Fig. 1, containing a 'nonporous' hydrophilic coating that is water permeable (chitosan), an electrospun nanofibrous support (PAN) and a non-woven microfibrous substrate (PET).

2. Experimental

2.1. Materials and preparation

Polyacrylonitrile (PAN) with a weight-average molecular weight (M_w) of about 1.5×10^5 g/mol and chitosan with a viscosity-based molecular weight (M_v) ranging between 1.9×10^5 and 3.1×10^5 g/mol were purchased from the Aldrich Chemicals. Dimethylformamide (DMF, Aldrich) and acetic acid (glacial, Fischer) were used as solvents for PAN and chitosan, respectively, without further purification. The poly(ethylene terephathalate) non-woven substrate (PET microfilter FO2413 with an average fiber diameter of about 10 μm) for membrane support was kindly provided by Freudenberg Nonwovens (Hopkinsville, KY).

PAN was dissolved in DMF at 50 °C and the solution was stirred for one day or a sufficiently long period of time until it became homogenous. Polymer solutions of several different concentrations were prepared, ranging from 4 to 12 wt%. Chitosan was purified before use by the following procedure. The chitosan sample (~1 g) was dissolved in acetic acid (1 wt%) and the solution was filtered using a nonporous medium sintered glass filter to remove insoluble substance. The solution was subsequently cast in a plastic petri dish and left in the fume-hood to dry. The dried chitosan film was then soaked in sodium hydroxide solution (concentration: 1 M) for a few hours. After peeled off, the films were washed by deionized water until neutralized. The neutralized films were freeze-dried for 24 h before use. With the purified chitosan sample, the coating solutions were prepared at a concentration range from 0.5 to 1.2 wt% in acetic acid solution (1 wt%). The solution pH was adjusted to ~6.5 by 1 N sodium hydroxide.

2.2. Fabrication of three-tier composite membrane

The non-woven PET micro-filter substrate was first primed with a 1 wt% chitosan solution to enhance its adhesion with electrospun PAN nanofibers. In this process, about 2 ml of chitosan solution was used to prime the sample with 7.6×10.2 cm^2 cross-section area (the total amount of pre-coated chitosan was about 20 mg). The PAN solution (4–12 wt% in DMF) was electrospun directly onto the surface-coated PET non-woven substrate at 14–20 kV. The flow rate was 10–20 μl/min and the spinneret diameter was 0.7 mm. The distance between the collector (PET substrate) and the spinneret was 10–18 cm, depending on the polymer concentration. In the electrospinning setup, a rotating metal drum with the diameter of about 9 cm and a rotating speed of about 300 rpm was used to collect the deposited nanofibers. A stepping motor was used to control the oscillatory translational motion perpendicular to the drum rotation direction (the oscillation distance was about 12 cm) to ensure the production of uniform electrospun scaffolds with sufficient membrane area (i.e. larger than 7.6×10.2 cm^2). The typical amount of PAN nanofibers spun per unit area was about 1.2 mg/cm^2. In addition to electrospinning of a solution at a fixed polymer concentration, the following procedure was also used to fabricate asymmetric scaffolds consisting of two multi-layers of fibers having different fiber diameters. The first multi-layer was produced by using a 10 wt% or higher polymer concentration solution, resulting in a larger fiber diameter; the second multi-layer was produced by using a 4 wt% solution, resulting in a smaller fiber diameter. The finer and denser fibrous structure on top was designed to support a thinner layer of coating that could withstand the desired operating pressure for the filtration process.

The coating layer was applied onto the fibrous composite support containing electrospun PAN scaffold and non-woven PET substrate by cast-coating with a chitosan solution (concentration: 0.5–1.4 wt%, pH 6.5). To ensure the creation of a relatively smooth chitosan layer on the surface of PAN scaffold, the following procedure was used. The scaffold was first soaked in 1 N NaOH solution before coating to minimize the penetration of chitosan solution into the PAN nanofibrous support. The resulting three-tier composite membrane was dried for one day under ambient conditions. The dried membrane was then washed with water until the membrane became completely neutralized. The total thickness of chitosan/PAN layer (excluding the non-woven PET substrate) was about 60 μm after drying.

2.3. Characterization

The structures of the top-layer coating, the electrospun mid-layer support and the cross-section of the coating/nanofibrous support interface were examined by scanning electron microscopy (SEM, LEO 1550) equipped with Schottky field emission gun (10 kV) and Robinson backscatter detector. All specimens received 24 s of gold coating to minimize the charging effect. The fiber diameter and pore area were measured by the Scion® image analysis program after calibration with standards.

The feed solution was prepared by mixing of vegetable oil (1350 ppm), surfactant (150 ppm, Dow Corning 193 fluid) and deionized water. A custom-built cross-flow filtration cell (active filtration area: 0.00652 m^2) was used to test the filtration performance of composite membranes. The chosen trans-membrane pressure (Δp) was 50 psi and the chosen inlet pressure was 130 psi, which was maintained constant throughout the entire experiment. The chosen operating temperatures were 30–33 °C. The flux measurements were repeated three times to confirm the performance of each sample.

The filtration efficiency of the composite membrane was determined as follows. The surfactant concentrations of the initial feed solution and the filtered liquid (permeate) were determined by ultraviolet–visible (UV) spectroscopy (BioRad SmartSpec 3000) at a wavelength of 230 nm (i.e. in the range of 150–0 ppm oil–surfactant mixture). The rejection percent was calculated by using the following equation.

$$\text{Rejection } (\%) = \frac{(C_f - C_p)}{C_f} \times 100 \quad (1)$$

where C_f and C_p represent the surfactant concentration of the feed solution and that of the permeate, respectively.

3. Results and discussion

3.1. Electrospinning of PAN nanofibrous support

Although there are many parameters in electrospinning (e.g. flow rate, applied electric field, and distance between spinneret and collecting drum) that can be used to control the fiber diameter, our previous study showed that one of the most effective schemes to alter the fiber diameter was to change the solution concentration [30]. This finding was also confirmed in the present study. By changing the PAN concentration from 4 to 12 wt% while keeping other processing parameters constant, the average fiber diameter could be varied from 124 to 720 nm, as shown in Fig. 2. Furthermore, the fiber diameters at higher concentrations (i.e. more than 10 wt%) appeared to approach a constant value (~750 nm) under our experimental conditions. Fig. 3 shows the corresponding SEM images of PAN fibers electrospun at different concentrations, clearly illustrating that all the fabricated fibers showed fairly good uniformity. The average diameter was found to increase with the solution concentration.

3.2. Surface porosity of electrospun scaffold

Commercial image analysis software was used to determine the surface porosity of electrospun membranes as well as those of commercial UF/NF filters. The results are shown in Fig. 4. The electrospun membrane based on the 4 wt% of PAN solution exhibited the highest porosity value (~73%), which was significantly higher than the values determined from

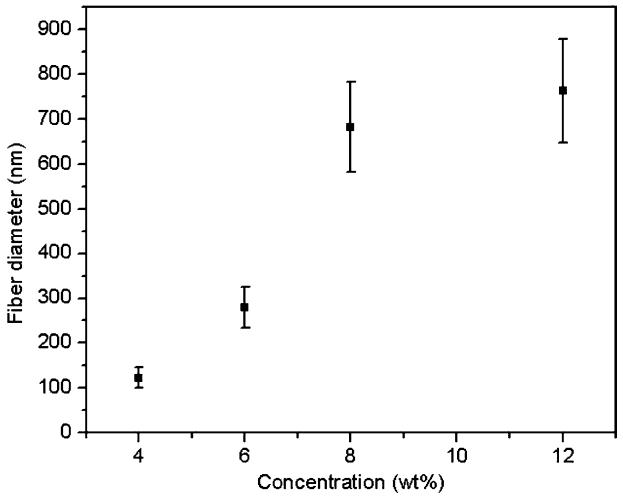

Fig. 2. Changes in electrospun PAN fiber diameter with polymer solution concentration (4–12 wt%).

commercial UF (e.g. Pall Corporation) and NF (e.g. Amicon XM300) filters and more than 2 times larger than that of Millipore HAWP microfiltration filter (~34%).

The different nature of surface porosity between the conventional ultrafiltration filter (e.g. an UF filter from Pall Corporation) based on the porous membrane format and the electrospun scaffold can be clearly seen from the tilted view of processed image by the image analysis program (Fig. 5). It is noted that while the surface porosities in UF and NF filters are quite similar, they are very different from the bulk porosity. In Fig. 5, the processed surface SEM images exhibited the surface structure of the dense top layer, resulted from the solvent evaporation process near the membrane surface during the phase inversion procedure [6]. However, the surface porosity of an electrospun PAN scaffold was found to be very close to its bulk porosity. The porosity appeared to be related mainly to the fiber diameter–since we have not tried to fine-tune the fiber number density. The SEM images showed that variations in the fiber diameter could change the porosity under our experimental conditions. If we assume that the pore geometry could be described by the Hagen-Poiseuille model and the surface porosity of the membrane was close to its bulk porosity, then the surface porosity could be correlated to the flux by using the following equation [31].

$$J_w = \frac{r_p^2 \Delta P}{8\mu(\Delta x/A_k)} \tag{2}$$

where J_w represents the flux (m/s), r_p represents the effective pore radius (m), ΔP represents the applied pressure drop

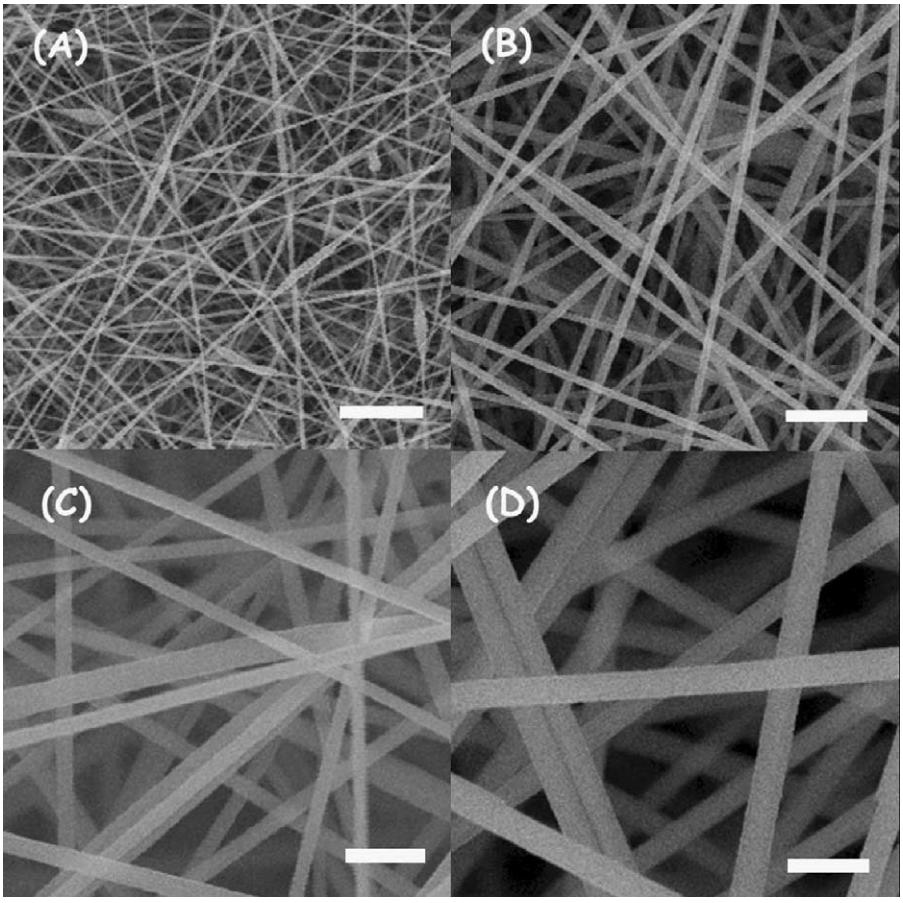

Fig. 3. Scanning electron microscope (SEM) images of electrospun PAN nanofibrous scaffolds using solutions of (A) 4 wt%, (B) 6 wt%, (C) 8 wt% and (D) 12 wt%. All scale bars are 2 μm.

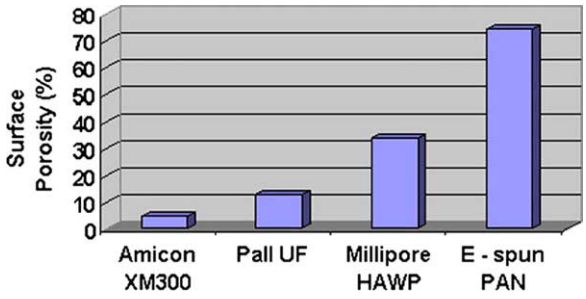

Fig. 4. Surface porosity of conventional ultrafiltration membrane (e.g. Amicon XM300) and nanofibrous support (the porosity was measured by electron microscopyimages).

(kN/m^2), μ is the viscosity of solution (Pa s), Δx is the effective membrane thickness (m) and A_k is the porosity of the membrane. Here, the flux is taken to be proportional to the surface porosity. For practical oily water ultrafiltration, a more complex expression with additional parameters should be used. However, Eq. (2) has provided us a simple guideline to correlate the flux performance with surface porosity. It also illustrated that the electrospun nanofibrous scaffold should have a much higher flux than conventional nonporous membranes in UF or NF filters.

3.3. Three-tier composite membranes for ultrafiltration

Although electrospun scaffolds can be considered as effective filters for liquid filtration, there is a major drawback for practical use of these materials by themselves, i.e. the high surface porosity of the electrospun nanofibrous scaffold will lead to a high-fouling problem. The symptom of fouling is an unavoidable consequence of gradual blockage of permeation in the membrane during filtration. The fouling rate is a function of many variables (e.g. the surface characteristics of the membrane, the surface-to-volume ratio of the membrane, the flow rate, the permeant concentration, the filtration temperature, the character of feed and reentrant streams), where the surface characteristics play a major role. The high fouling rate indicates that the replacement frequency must be high, resulting in an effective correspondingly higher operational cost.

A thin layer of hydrophilic but water resistant, nonporous, but water permeable, chitosan coating was deposited onto the nanofibrous PAN surface to minimize the fouling concern. The chitosan coating would allow water to penetrate without losing too much flow rate, while the smooth coating surface would minimize the blockage problem. Moreover, in order to support a uniform chitosan coating, an asymmetric structure of nanofibrous support that had two multi-layers of different fiber diameters was constructed. The asymmetric structure possesses: (1) a multi-layer of finer fiber diameter with lower porosity to support the coating, (2) a multi-layer of larger fiber diameter with higher porosity to interface the transition with the non-woven PET substrate. Our reasons are as follows. It is known that the volumetric flow rate is inversely proportional to the thickness of nonporous top coating layer, which obeys D'Arcy's law [6]

$$J = KP/(\eta L) \tag{3}$$

where K is the hydraulic permeability of the membrane, η is the viscosity of the liquid, L is the thickness of the membrane and P is the pressure. Thus, the thinner the coating layer, the higher the flux. In order to apply a thin coating layer on top of the electrospun scaffold, finer fiber diameter and denser structure could better maintain the coating surface uniformity. Based on experimental results from electrospinning of varying PAN solutions, the scaffold generated by the 4 wt% solution was found to have the smallest fiber diameter (Figs. 2 and 3). Our strategy to produce a three-tire composite membrane having an *asymmetric* nanofibrous PAN support is illustrated in Fig. 6, where the asymmetric support was fabricated by sequential electrospinning of 12 and 4 wt% solutions, respectively. The thickness of the scaffold produced by the 4 wt% solution was estimated to be the order of micrometers from the cross-section SEM image of composite membrane. Even with the pre-rinsing procedure (using 1 N NaOH solution), the chitosan coating layer could still penetrate into several nanofibers (with a mean diameter of about 124 nm). Fig. 7 shows SEM images of the surfaces of each layer: non-woven PET substrate, electrospun asymmetric PAN scaffold (from sequential process of 12 and 4 wt% solutions) and chitosan coating layer. Schematic diagrams of the cross-sectional assembly and a typical SEM image of fractured cross-sectional view of the assembled membrane are shown in Fig. 8. From SEM observations, the surface of the chitosan coating layer seemed to be smooth and flat, and the coating thickness was about 1 μm. With different chitosan concentrations, the thickness of the coating layer

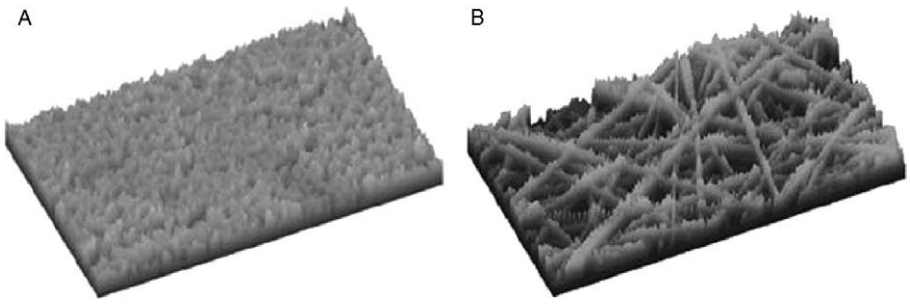

Fig. 5. Surface plots for (A) Pall UF membrane (B) 4 wt% PAN e-spun membrane.

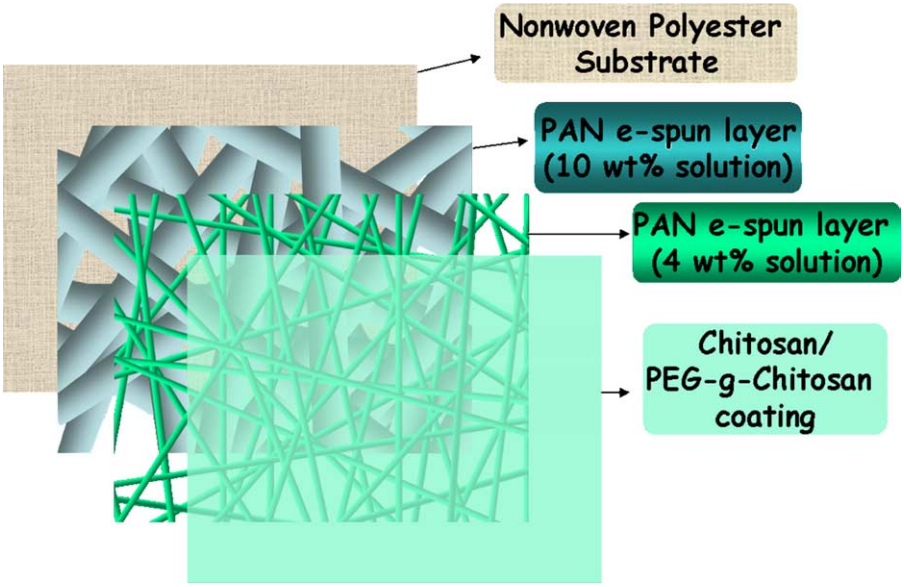

Fig. 6. Schematic diagrams for the assembly of three-tier composite membrane.

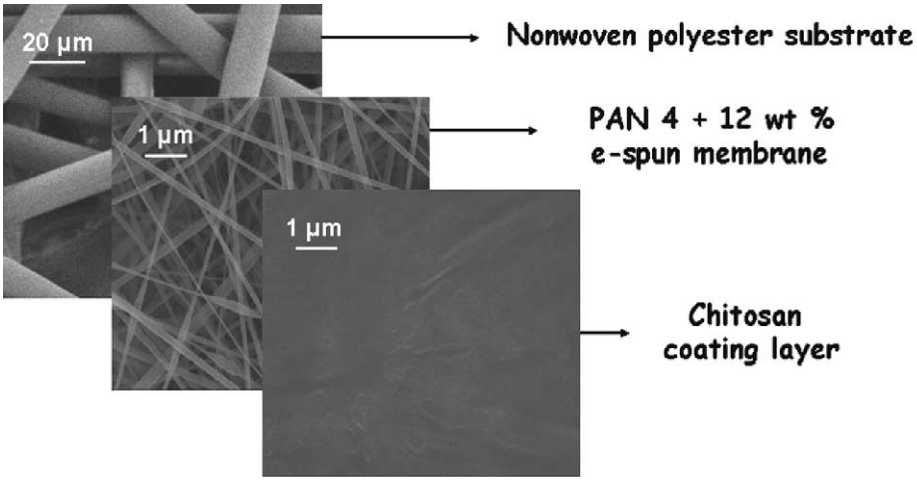

Fig. 7. SEM images of each layer in the three-tier composite membrane for ultrafiltration.

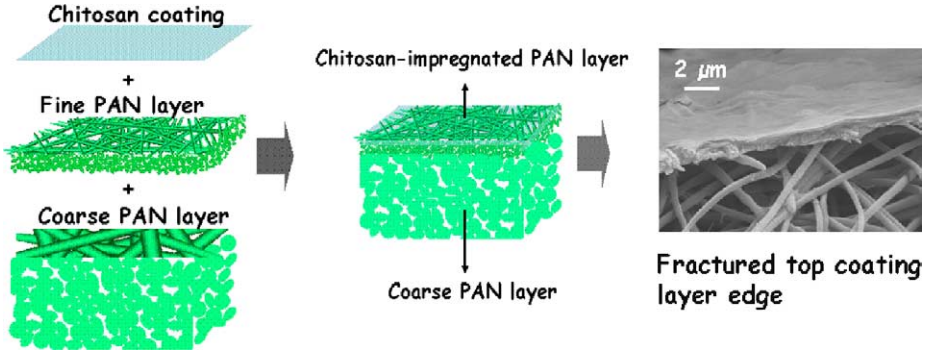

Fig. 8. Fabrication schematics of the electrospun scaffold with a coating layer. SEM image represents the fractured composite membrane containing PAN nanofibrous scaffold (with 4 + 12 wt% sequential electrospinning) and chitosan coating.

could be changed from 1 to 3 μm. It is noted that the thickness of the top coating layer is of crucial importance to the performance of the filter. Its optimization that also depends on the applied pressure, the structure of the asymmetric mid-layer, and durability, has not yet been carried out. Further study is in progress.

3.4. Evaluation of filtration performance

Based on the cross-flow ultrafiltration measurement, we found that the chitosan/PAN/PET three-tier composite membranes, although not yet fully optimized, showed much higher average flux rates than commercial UF and NF filters. A comparison among two composite membranes with different chitosan coating thicknesses (one about 1.3 μm by coating of 1.37 wt% solution and one about 1 μm by coating of 1.2 wt% solution) and a commercial NF fiber (i.e. NF 270 from Dow) has been made and results are shown in Fig. 9. Both chitosan/PAN/PET three-tier composite membranes exhibited an order of magnitude higher flux rate than the chosen NF filter after 20 h of operation, and the chitosan layer having a thinner thickness exhibited a higher flux rate. In the chosen composite membranes, a thickness reduction of about 0.3 μm in the chitosan coating layer resulted in an approximate 30% increase in flux. This suggests that if the coating layer thickness can be reduced, the flux rate can be further increased. Over a measurement time of 24 h, all three systems showed a slow decrease in flux (i.e. 25% through the entire measurement time), which could be attributed to the fouling problem, i.e. irreversible accumulation of oily particles and emulsions on the membrane surface. However, it should be noted that the initial decrease in flux (<1 hr) was not due to fouling, but due to the compression of nanofibrous scaffolds under pressure, which decreased the effective bulk porosity and retarded the water transportation. It is conceivable that the two approaches can be used simultaneously to improve the membrane performance (higher flux and lower fouling): (1) cross-linking of chitosan layer by glutaraldehyde, and (2) grafting of more hydrophilic polyethylene glycol molecules on the chitosan chains. Further studies are under way.

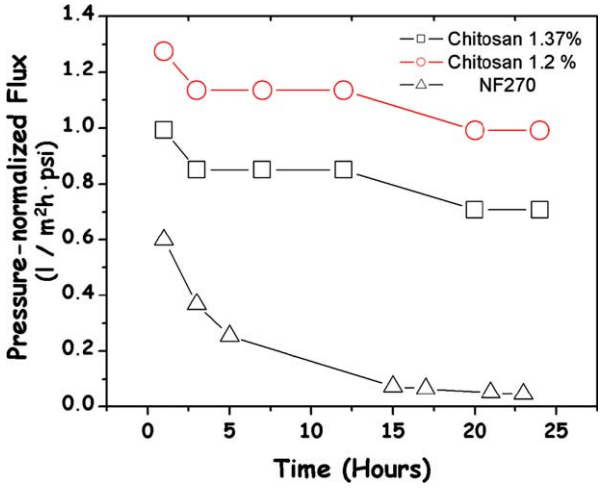

Fig. 9. The flux performance of the three-tier composite membranes with coating of 1.37 and 1.2 wt% chitosan solutions on an asymmetric electrospun PAN support, respectively as well as the commercial NF filter (Dow NF270) for filtration of oily waste water (1350 ppm of vegetable oil + 150 ppm of DC 1193 fluid + water). The operation conditions were as follows: the inlet pressure was 130 psi and the temperature was 30–33 °C.

Table 1
Rejection efficiency of oily waste water in ultrafiltration by different membranes

	Rejection (%)	Concentration (ppm)
NF 270	99.4	8.5
Three-tier composite membrane[a]	>99.95	<0.82

[a] PAN asymmetric nanofibrous support + chitosan coating (1.2 wt%) composite membrane.

Under the chosen testing conditions (130 psi, 30–33 °C), the filtration efficiency of the three chosen filtration systems was also measured by monitoring the surfactant concentration of the feed solution and that of the permeate. Results are shown in Table 1. Both chitosan/PAN/PET three-tier composite membranes showed similar filtration efficiency with a rejection ratio of greater than 99.9%. This value was even slightly better than that of NF 270, which was 99.4%. This indicates that the chitosan/PAN/PET three-tier composite membrane filtration system can be further optimized to increase the flux rate without sacrificing the filtration efficiency.

4. Conclusions

A new type of high flux ultrafiltration or nanofiltration composite membranes containing a thin layer of hydrophilic but water-resistant chitosan coating, an asymmetric electrospun PAN nanofibrous mid-layer support and a non-woven PET substrate was demonstrated. By nature, the electrospun nanofibrous support possesses a highly interconnected pore structure throughout the entire mid-layer scaffold thickness (the porosity can be larger than 70%), which is very different from that of conventional asymmetric porous membranes with a porosity only in the range of 34%. To support the thin layer of chitosan coating, an asymmetric electrospun support with finer fiber diameter for the coating surface was produced by sequential electrospinning of two different polymer concentrations. Three-tier composite membranes exhibited flux rates that could be over an order of magnitude higher than the commercial nanofiltration filter (e.g. NF 270 from Dow) after 24 h operation, while they maintained good filtration efficiency with rejection ratios better than 99.9% (i.e. less than 1 ppm in the permeate). It is important to point out that the demonstrated composite membranes have not been fully optimized for further improvements. It is conceivable that with additional modifications of the top coating layer (e.g. PEG-grafted chitosan and other hydrogels) and the reduction of coating layer thickness, the flux rate and the fouling problem can be further improved.

Acknowledgements

The financial support of this work was provided by the Office of Naval Research (N000140310932). The authors acknowledge the helpful assistance of Dr Richard F. Salinaro from the Pall Corporation for the construction of the cross-flow ultrafiltration cell.

References

[1] Smorada R. Encyclopedia of chemical technology. New York: Wiley; 1996.
[2] Mayer E, Warren J. Filtr Sep 1998;35:912.
[3] Hajra MG, Mehta K, Chase GG. Sep Purif Technol 2003;30:79.
[4] Graham K, Gogins M, Schreuder-Gibson H. Int Non-wovens J 2004;13:21.
[5] Schreuder-Gibson HL, Gibson P, Senecal K, Sennett M, Walker J, Yeomans W, et al. Adv Mater 2002;34:44.
[6] Zeman LJ, Zydney AL. Microfiltration and ultrafiltration. New York: Marcel Dekker, Inc.; 1996.
[7] Gibson P, Schreuder-Gibson H, Rivin D. Colloids Surf A Physicochem Eng Aspects 2001;187–188:469.
[8] Shin C, Chase GG. AICHE J 2004;50:343.
[9] Zong XH, Li S, Chen E, Garlick B, Kim KS, Fang D, et al. Ann Surg 2004;(240):910.
[10] Jia HF, Zhu GY, Vugrinovich B, Kataphinan W, Reneker DH, Wang P. Biotech Prog 2002;18:1027.
[11] Katti DS, Robinson KW, Ko FK, Laurencin CT. J Biomed Mater Res Part B: Appl Biomater 2004;70B:286.
[12] Wang X, Drew C, Lee SH, Senecal KJ, Kumar J, Samuelson LA. Nano Lett 2002;2:1273.
[13] Liu H, Kameoka J, Czaplewski DA, Craighead HG. Nano Lett 2004; 4:671.
[14] Jones Jr WE, Dong H, Nyame V, Ochanda F. Ann Tech Conf Soc Plast Eng 2003;2:1948.
[15] Fridrikh SV, Yu JH, Brenner MP, Rutledge GC. Phys Rev Lett 2003; 90:144502.
[16] Theron SA, Zussman E, Yarin AL. Polymer 2004;45:2017.
[17] Wrasidlo WJ, Mysels KJ. J. Parenteral Sci Technol 1984;38:24.
[18] Paulsen FG, Shojaie SS, Krantz WB. J Membr Sci 1994;91:265.
[19] Petersen RJ. J. Membr Sci 1993;83:81.
[20] Wang X, Chen X, Yoon K, Fang D, Hsiao BS, Chu B. Environmental Sci Tech 2005;39:7684.
[21] Wang X, Fang D, Yoon K, Hsiao BS, Chu B, J. Membrane Sci, 2005 in press.
[22] Musale DA, Kumar A, Pleizier G. J Membr Sci 1999;154:163.
[23] Musale DA, Kumar A. J Appl Polym Sci 2000;77:1782.
[24] Chandorilar MV, Bhavsar PC. Indian J Technol 1983;21:124.
[25] Wang Y, Serrano S, Santiago-Aviles JJ. Synth Met 2003;138:423.
[26] Kalayci VE, Patra PK, Buer A, Ugbolue SC, Kim YK, Warner SB. J Adv Mater 2004;36:43.
[27] Gudmund SB, Thorleif A, Paul S. Chitin and Chitosan: sources, chemistry, biochemistry, physical properties and applications. New York: Elsevier; 1989.
[28] Wang X, Spencer HG. J Appl Polym Sci 1998;67:513.
[29] Musale DA, Kumar A. Sep Purif Technol 2000;21:27.
[30] Zong X, Ran S, Fang D, Hsiao BS, Chu B. Polymer 2003;44:4956.
[31] Bowen WR, Hilal N, Lovitt RW, Sharif AO, Williams PM. J Membr Sci 1997;126:91.